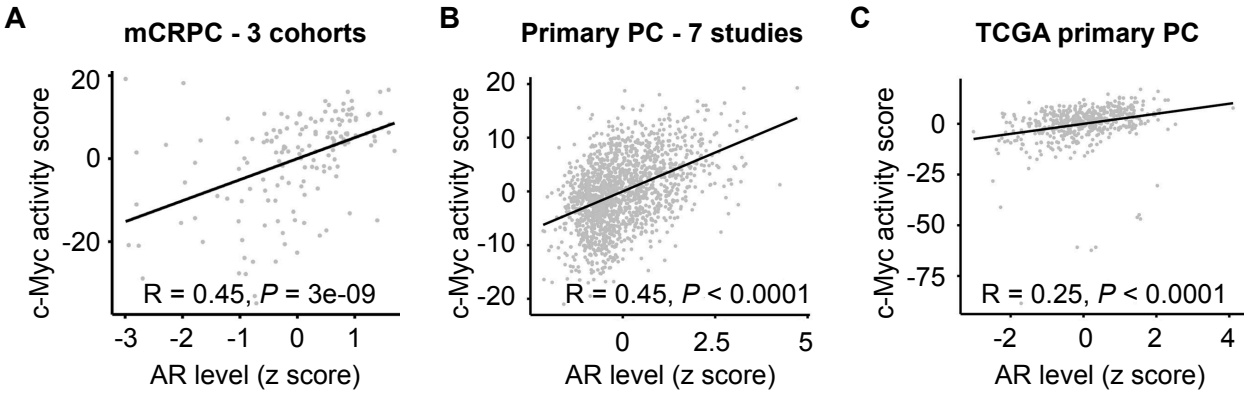

Figure S1. c-Myc activity determined using the the Jung c-Myc-target signature positively correlates with AR level in human prostate cancer samples. Pearson's correlation coefficient analysis showing a positive correlation between c-Myc activity score and AR level in 159 mCRPC samples from 3 cohorts **(A),** a meta dataset of 1642 primary prostate cancer samples **(B),** and the TCGA dataset of 500 primary prostate cancer samples **(C)**. The c-Myc activity score was computed as the sum of z-scores for the Jung c-Myc-target signature.

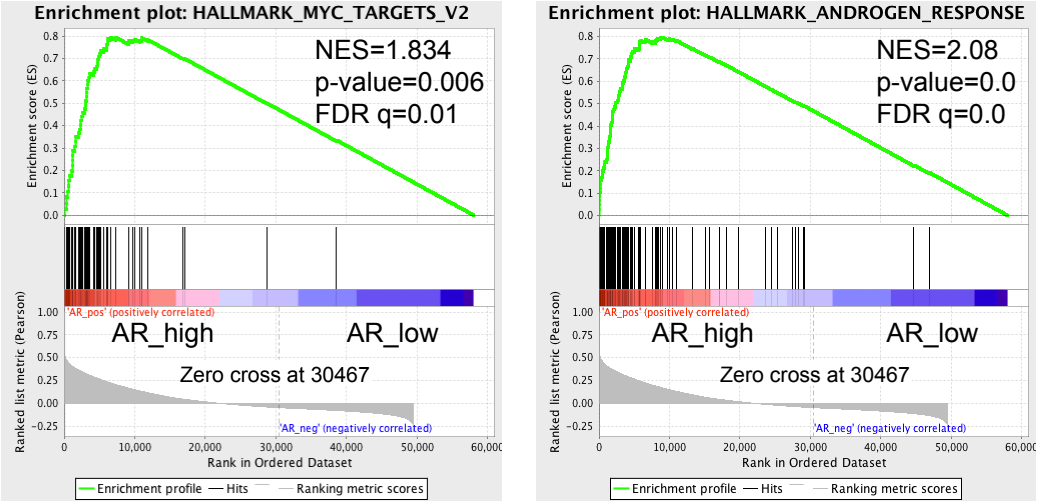

Figure S2. GSEA showing enrichment of the hallmark Myc_targets_v2 and androgen_response pathways in mCRPC samples (n = 159) that express a high level of AR.

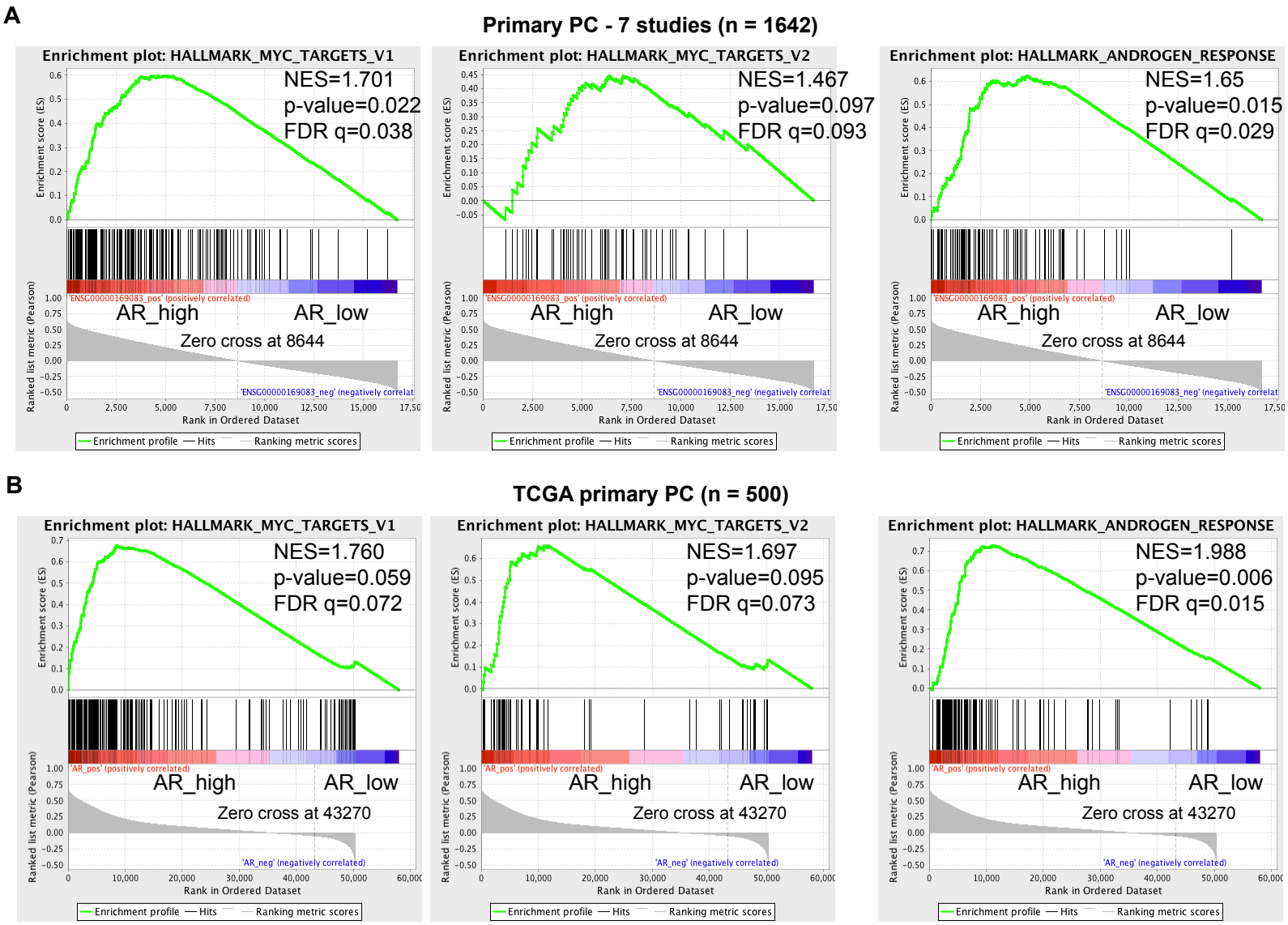

Figure S3. GSEA showing enrichment of the hallmark Myc_targets_v1, Myc_targets_v2, and androgen_response pathways in primary prostate cancer samples that express a high level of AR. A, a meta dataset of 1642 primary prostate cancer samples; **B,** the TCGA dataset of 500 primary prostate cancer samples.

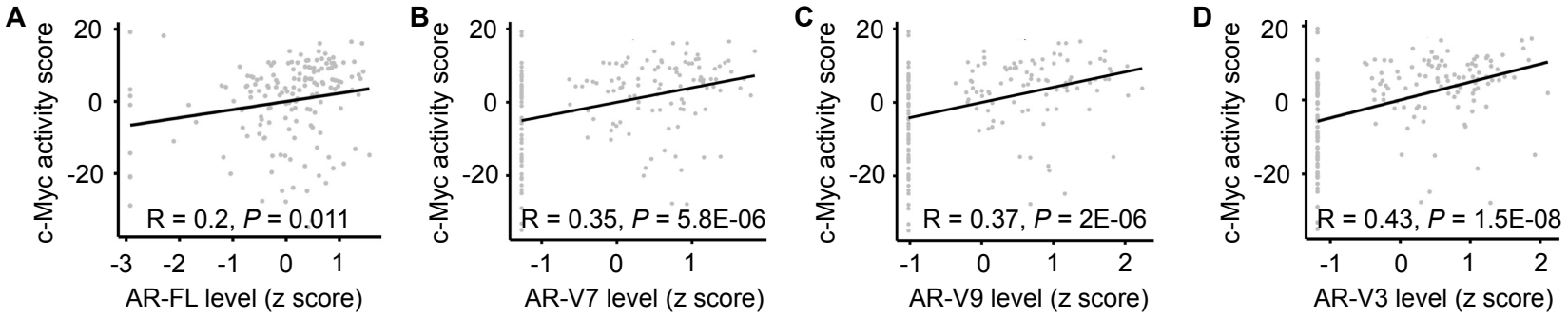

Figure S4. c-Myc activity, calculated using the Jung c-Myc-target signature, positively correlates with AR-FL, -V7, -V9, and -V3 levels in 159 mCRPC samples in Pearson's correlation coefficient analysis. The AR-FL, -V7, -V9, and -V3 levels were quantified as normalized number of RNA-seq reads spanning AR exons 7-8, 3-CE3, 3-CE5, and 2-CE4 splice junctions, respectively. The c-Myc activity score was computed as the sum of z-scores for the Jung c-Myc-target signature.

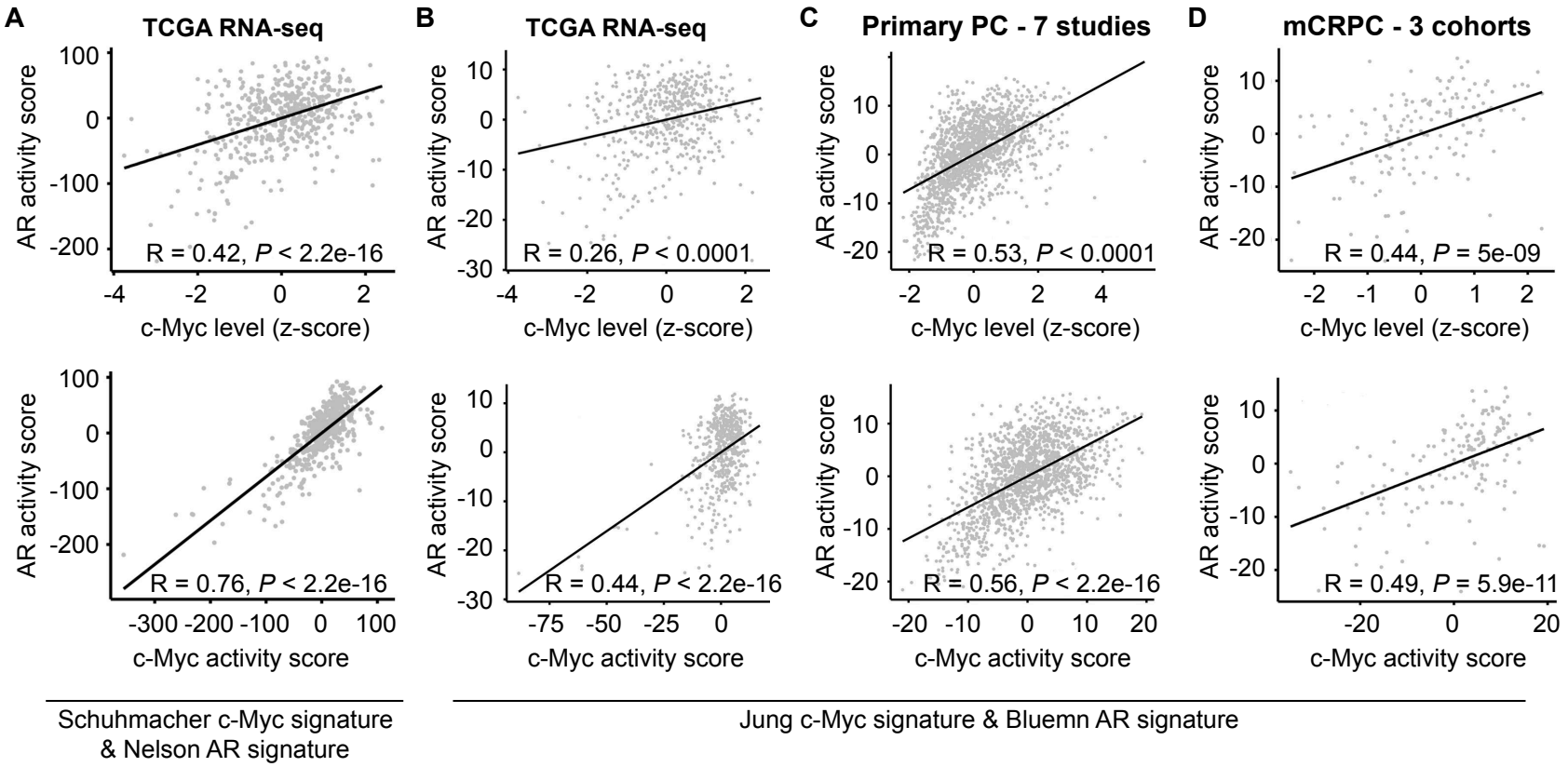

Figure S5. c-Myc level and activity positively correlate with AR activity in human prostate cancer samples. Pearson's correlation coefficient analysis showing a positive correlation between c-Myc level and AR activity score (top panels) and between c-Myc and AR activity scores (bottom panels) in the TCGA dataset of 500 primary prostate cancer samples (**A & B**), a meta dataset of 1642 primary prostate cancer samples **(C),** and 159 mCRPC samples from 3 cohorts **(D)**. The c-Myc and AR activity scores were computed as the sum of z-scores for the Schuhmacher c-Myc-target signature and the Nelson AR-target signature, respectively, in **A** and as the sum of z-scores for the Jung c-Myc-target signature and the Bluemn AR-target signature, respectively, in **B to D**.

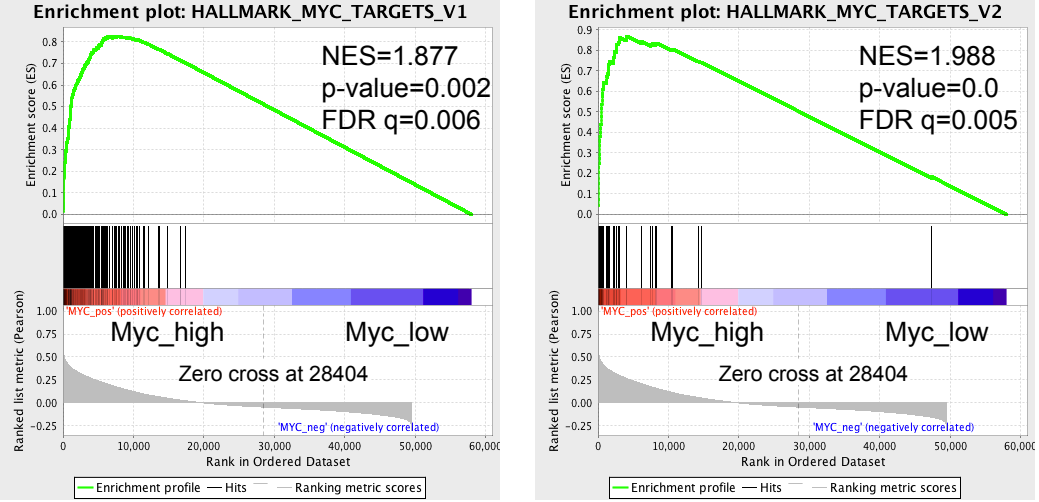

Figure S6. GSEA showing enrichment of the hallmark Myc_targets_v1 and Myc_targets_v2 pathways in mCRPC samples (n = 159) that express a high level of c-Myc.

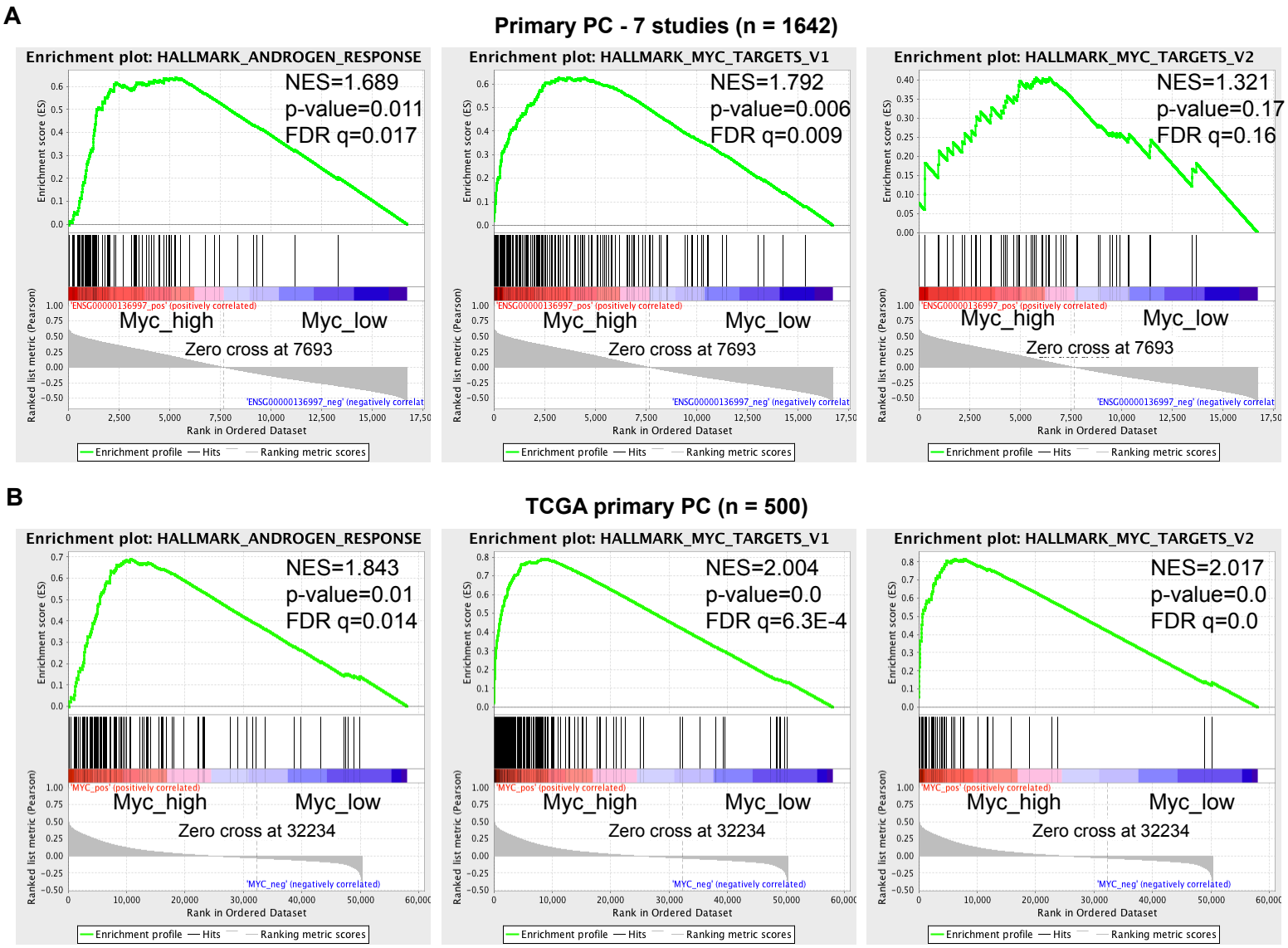

Figure S7. GSEA showing enrichment of the hallmark androgen_response, Myc_targets_v1, and Myc_targets_v2 pathways in primary prostate cancer samples that express a high level of c-Myc. A, a meta dataset of 1642 primary prostate cancer samples; **B,** the TCGA dataset of 500 primary prostate cancer samples.

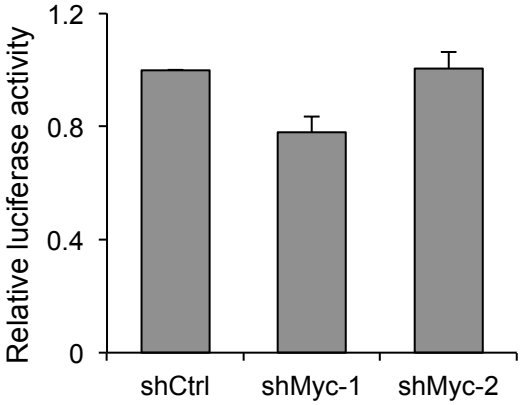

Figure S8. Knockdown of c-Myc does not affect CMV-promoter activity. Luciferase assay showing no change in CMV-promoter activity after c-Myc knockdown. At 24 h after shCtrl- or shMyc-lentivirus transduction, 22Rv1 cells were transiently transfected with the pGL4-CMV-Luc construct in bulk and reseeded in triplicate 24 h post transfection for luciferase assay.

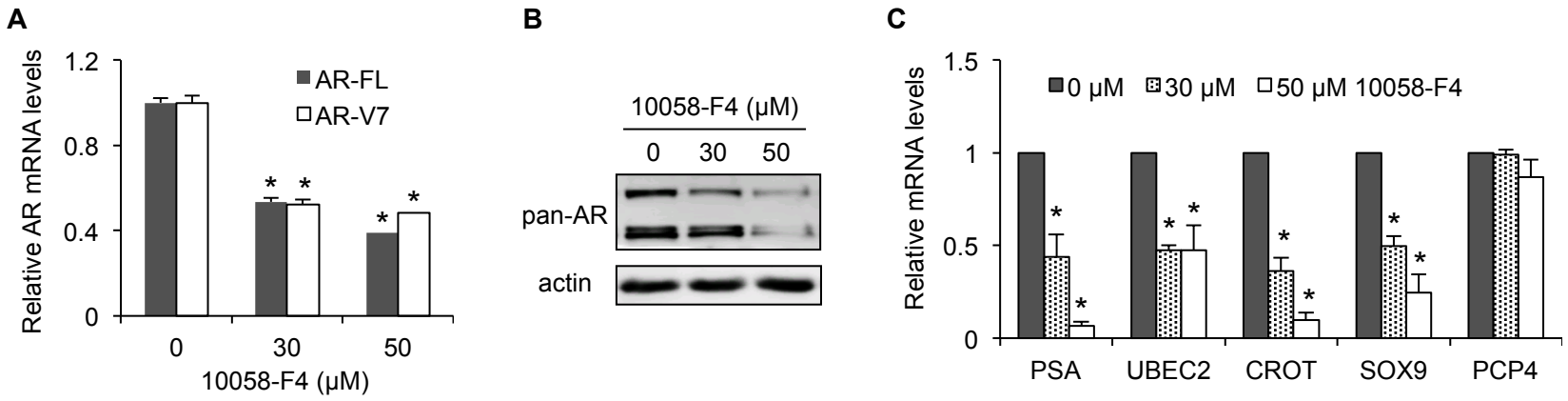

Figure S9. c-Myc inhibition leads to reduced expression of AR-FL and AR-V7 as well as their target genes. A and B, qRT-PCR (A) and Western blot analysis (B) showing a downregulated expression of AR-FL and AR-V7 mRNA and protein in 22Rv1 cells after treatment with the 10058-F4 c-Myc inhibitor. **C,** qRT-PCR analysis showing a reduced expression of AR-FL and AR-V7 targets, PSA, UBE2C, CROT, and SOX9, but not the non-AR target PCP4 in 22Rv1 cells after treatment with 10058-F4. *, $P < 0.05$ from the control cells.